

## Adhesion Strength of TiZrN/TiSiN Nanocomposite Coatings on a Steel Substrate with Transition Layer

V.M. Beresnev<sup>1</sup>, S.V. Lytovchenko<sup>1</sup>, B.O. Mazilin<sup>1</sup>, D.V. Horokh<sup>1</sup>, V.A. Stolbovoy<sup>1,2</sup>, D.A. Kolesnikov<sup>3</sup>, I.V. Kolodiy<sup>2</sup>, S. Zhanyssov<sup>4</sup>

<sup>1</sup> V.N. Karazin Kharkiv National University, 4, Svobody Sq., 61000 Kharkiv, Ukraine

<sup>2</sup> National Scientific Centre "Kharkiv Institute of Physics and Technology",  
1, Akademichna St., 61108 Kharkiv, Ukraine

<sup>3</sup> Belgorod National Research University, 85, Pobedy St., 308015 Belgorod, Russia

<sup>4</sup> D. Serikbayev East Kazakhstan State Technical University,  
69, Protozanov St., 070004 Ust-Kamenogorsk, Republic of Kazakhstan

(Received 11 May 2020; revised manuscript received 15 August 2020; published online 25 August 2020)

Influence of surface pretreatment on adhesion properties of TiZrN/TiSiN vacuum-arc coatings on steel substrates 12X18H9T has been studied. Multilayer coatings were obtained by spraying two cathodes of compositions (mass %) 75 Ti + 25 Zr and 94 Ti + 6 Si in the same technological cycle with pretreatment, which could include cleaning of samples with gas plasma in the two-stage gas discharge or ion bombardment at arc spraying of cathodes, deposition on the substrate at arc spraying of cathodes, as well as combinations of these variants of cleaning with substrates. X-ray analysis, electron microscopy, sclerometry and micro-hardness measurements were used to study the composition, structure and properties of the obtained "coating-substrate" composites. The features of deformation and degradation of coatings formed after different variants of preliminary preparation of samples were revealed. Values of critical loads at dynamic indentation of coatings, changes in friction coefficient and level of acoustic emission signal testify to high adhesive strength of (TiZr)N/(TiSi)N coatings, which allows recommending them to increase cutting tool performance. The presence of an intermediate layer does not increase the resistance of these coatings to breakage, but it slows down the process of degradation of coatings and smooths sharp jump changes in properties.

**Keywords:** Vacuum-arc coatings, Adhesive strength, Multilayer coatings, Preliminary preparation, Plasma heating, Intermediate layer.

DOI: [10.21272/jnep.12\(4\).04030](https://doi.org/10.21272/jnep.12(4).04030)

PACS numbers: 61.46 – w, 62.20.Qp,  
62.23.Pq, 62.25. – g

### 1. INTRODUCTION

At present, solid ion-plasma multi-component and multilayer coatings based on various nitrides and carbonitrides of transition metals are used to improve the properties of tool materials and improve performance, in particular, the resistance to abrasion and other tribological characteristics, parts of machines and mechanisms [1, 2]. At the same time, it is known that the size of the adhesive bond of the surface film with the substrate determines the expediency of application of a coating in a particular area, while in most cases good adhesion contributes to improving the performance of cutting tools and extends their life [3]. In practice, the criterion for evaluating the adhesion of a coating is its adhesive strength, which is determined by the amount of work or applied force sufficient to tear the adhesive off the substrate. Adhesive interaction of functional film coatings with substrates has a fundamental effect on the application of nanocomposite coatings to improve the performance of products, and therefore much attention has been paid to improving adhesion between coatings and substrate materials. For example, vacuum-arc deposition of the transition layer between the coating and the substrate allowed to increase the adhesion strength of TiAlSiN coating [4]. Applying a transition layer or creating a multilayer structure can be considered as an alternative approach to improve adhesion in the "film-substrate" system, but both the expediency of the transition layer formation and the impact of its composition and structure on the adhesive

strength of coatings require more detailed study.

In the present work, the influence on adhesive strength of different variants of substrate surface pretreatment in a single technological process with the formation of TiZrN/TiSiN nanocomposite coatings was studied.

### 2. OBTAINING COATINGS AND RESEARCH METHODS

Samples of substrates were cut out of 12X18H9T sheet steel (sample size 15 mm × 15 mm, thickness 2.5 mm). After mechanical, chemical and plasma-electrolyte polishing [5] the surface quality for the formation of the coating corresponded to the purity class V14a. The samples were fixed on a special holder in the chamber of the modernized cathode arc deposition unit (Arc-PVD), the scheme of which is given in [6], with two composition cathodes (%) 75 Ti + 25 Zr and 94 Ti + 6 Si. To study the effect of substrate pre-preparation on the adhesive strength of coatings three series of samples were manufactured, pretreatment of which was carried out according to three different technological schemes:

– scheme 1: samples of series 1 were treated for 5 min in plasma of two-stage gas discharge at nitrogen pressure of 0.1 ... 0.2 Pa and negative potential on the substrate of about 1 kV;

– scheme 2: series 2 samples were first ion bombarded at high vacuum with arc evaporation of cathodes and negative potential on samples of 1 kV. Then the potential was reduced to 150 V and an intermediate layer (substrate) was deposited from cathode ions on the sur-

face for 5 min.

– scheme 3: samples of series 3 combined processing in gas plasma according to scheme 1 and the formation of a sublayer according to scheme 2.

Subsequent formation of coatings on pre-prepared samples of substrates was carried out by spraying two cathodes of the above compositions, with the substrate holder rotating at a rate of 8 rpm to move the samples alternately from one cathode to another. Nitrogen pressure  $P_N$  on the coating was 0.5 Pa and the negative displacement potential  $U_b$  on the substrates was maintained at 110 V. The cathode arc current was 85 A for TiZr and 100 A for TiSi. The duration of coating formation was 60 min.

Structural and phase analysis of the samples was carried out by X-ray diffractometry at DRON-4 unit in  $K_\alpha$  radiation of copper anode using nickel filter. Calculation of substructural characteristics (size of the coherent scattering region (CSR) and level of microdistortions  $\varepsilon$  of the crystal lattice) was performed by the Williamson-Hall method using the integral width of diffraction lines. Silicon powder with a grain size of  $\sim 30$  microns was used as a reference sample to account for the instrumental line widening. To determine the elemental composition of the coatings Quanta 200 3D electron-ion scanning microscope was used with an energy dispersion analyzer based on Si-Li X-ray sapphire detector. Surface topography was studied with a scanning microscope FEI Quanta 600 FEG.

Coating thicknesses were measured using electron-microscopic images of grinding of their cross sections, for the manufacture of which the equipment complex of Struers company was used. The surface of the samples was successively ground and polished on abrasive SiC paper with grit size from 320 to 4000 grit, then on the DiaDuo-2 diamond suspension with  $3\ \mu\text{m}$  and  $1\ \mu\text{m}$  particles. The grinding surface preparation was completed with polishing on OP-S oxide suspension. Immediately before the study, the polished samples were plasma cleaned in the Fischione Model 1020 for 20 min.

Adhesion strength and scratch resistance of coatings were determined by sclerometry with simultaneous registration of acoustic emission (AE) signals. This method and various scratch testers are widely used to determine the adhesion characteristics of films and coatings, their brittleness, plasticity, deformation, peeling as well as fracture features [7, 8]. The method is based on continuous loading of the investigated material with an indenter [9], which moves horizontally along the sample surface. Under such loading (scratching) the specimen is deformed in elastic and plastic regions to the limiting state with the subsequent destruction of the specimen. The Revetest scratch tester by CSM Instruments with a diamond spherical indenter of Rockwell C type with a radius of  $200\ \mu\text{m}$  was used in this work. Researches were carried out in a mode with progressive loading on an indenter (normal force  $N$  linearly increases to the set maximum value) from 0.9 N to 190 N. In this mode, the critical load is defined as the normal force at which the first cohesive and first adhesive damage is observed. The length of the scratch was 12 mm.

Simultaneously with the AE signal intensity registration, the loading parameters (normal load  $N$ ) and friction coefficient were recorded. The process can be monitored visually thanks to the integrated metallographic microscope. Two scratches were applied to the surface of each coated sample for better accuracy of the results.

The coating hardness was determined on the Shimadzu ultra microhardness meter at 50 mN.

### 3. RESULTS AND DISCUSSION

The images of the side cross-sections of the coatings of the samples of series 1 and 3, pre-treated according to the schemes 1 (purification in gas plasma) and 3 (purification in gas plasma with layer application), respectively, are shown in Fig. 1. Image analysis confirms rather high homogeneity and low defect thickness of the coatings. At the selected parameters of the image, the sublayer in Fig. 1b is visually indistinguishable. The image of the cross-section of the samples of series 2 (ion bombardment from cathodes and application of the sublayer) practically does not differ from the given ones.

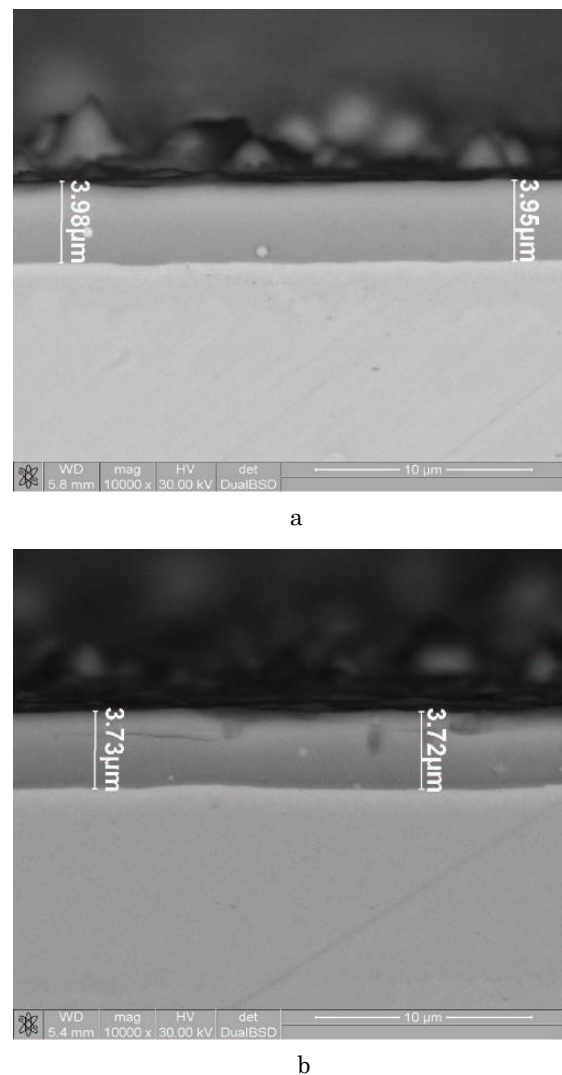


**Fig. 1** – Lateral cross-sections of the (TiZr)N/(TiSi)N coatings obtained at  $P_N = 0.5$  Pa and  $U_b = -110$  V with pretreatment in gas plasma: a) without substrate; b) with substrate

Data on the elemental composition of the coatings obtained from the processing of energy dispersion spectra are given in Table 1.

**Table 1** – Elemental composition of (TiZr)N/ (TiSi)N coatings

Series	Elemental composition of coatings, at. %			
	N	Ti	Zr	Si
1	44.25	49.88	5.02	0.85
2	43.33	50.40	5.44	0.83
3	43.30	50.13	5.75	0.82

The results show that pretreatment with the application of an underlay when treating the surface with both plasma and a beam of metal ions (series 2 and 3) leads to a slight decrease in Si concentration and an increase in the concentration of metal components Ti and Zr. The latter, of course, is due to the fact that the metals in the coating are associated with nitrogen in nitrides. This is confirmed by X-ray phase analysis data.

Analysis of diffraction spectra indicates the presence in the coating of 2 phases –TiZrN and TiN nitrides. In the spectrum, there are lines from the substrate, which is natural for these coating thicknesses and the selected energy of the X-ray beam. The lattice of TiZrN nitride is 0.4391 nm, the substructural characteristics of this phase could not be determined. The parameter of the TiN nitride lattice is 0.4320 nm, the size of the CSR of this phase is  $D = 24.2$  nm at the micro-distortion level  $\varepsilon = 5.76 \times 10^{-3}$ . The intensity analysis and structural analysis data (Fig. 2) indicate an advantageous texture growth  $\langle 111 \rangle$ . This structure contains titanium, zirconium, silicon and nitrogen (Table 1), which makes it possible to form nitrides based on titanium and zirconium. Silicon nitride phases were not detected. The spectrum shown here is obtained from the sample of series 1, spectra from samples of series 2 and 3 do not have significant differences from the spectrum shown here.

The results of determination of mechanical characteristics of the obtained (TiZr)N/(TiSi)N coatings are given in Table 2. In addition to hardness  $H$ , to describe the mechanical properties of coatings we used effective Young modulus  $E$  ( $E = E_{def}/(1 - \nu^2)$ , where  $E_{def}$  is the normal elastic modulus (Young modulus),  $\nu$  is the Poisson's coefficient), as well as the ratios  $H/E$ ,  $H^3/E^2$ .

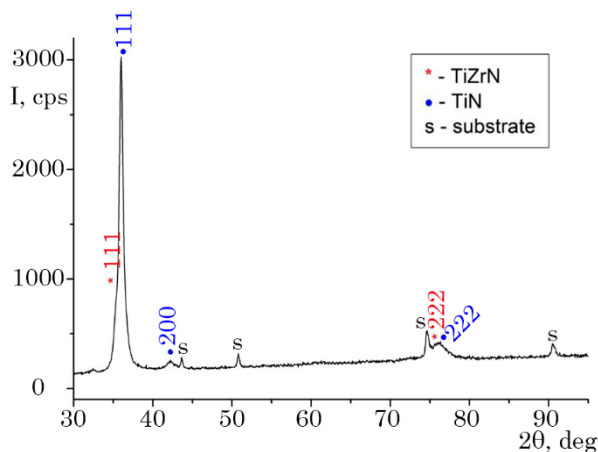


**Fig. 2** – Diffraction spectrum section of (TiZr)N/(TiSi)N condensate, sample of series 1

**Table 2** – Hardness and modulus of elasticity of (Ti Zr)N/(TiSi)N nanocomposite coatings

Series	Mechanical characteristics of coatings			
	$H$ , GPa	$E$ , GPa	$H/E$	$H^3/E^2$ , GPa
1	33	246	0.13	0.59
2	25	219	0.11	0.32
3	35	260	0.13	0.63

According to the classical theory of abrasive wear, wear resistance is directly proportional to hardness [10, 11]. This statement is true in many cases for metals, but already for alloys it is broken, and for many modern materials, including composite film coatings, the wear resistance of the material is proportional to the  $H/E$  ratio [12, 13]. Hence, at creation of wearproof materials it is necessary to aspire to combine high hardness with rather low modulus of elasticity that is easier to realize in coatings with horizontal-layered architecture. The value of  $H/E$ , sometimes called the plasticity index of the material, characterizes the elastic deformation of failure [14]. High values of this relation also testify to the increased wear resistance of the coating. To an even greater extent, the plastic deformation resistance, according to the indentation data, defines the value of  $H^3/E^2$ , which can be used to predict the behavior of the material under mechanical loads: the increase in the resistance of the material elastic deformation of failure and reduction of plastic deformation of the material is achievable at its high hardness and low modulus of elasticity [15-17].

The data of Table 2 show that the maximum value of microhardness in the obtained coatings is equal to  $H = 35$  GPa and elastic modulus is  $E = 260$  GPa. The analysis of  $N/E$  dependences for different materials [18] has allowed to establish that the obtained coatings (TiZr)N/(TiSi)N can be attributed to the group of materials which are in amorphous and amorphous-nanocrystalline states ( $H/E \geq 0.1$ ).

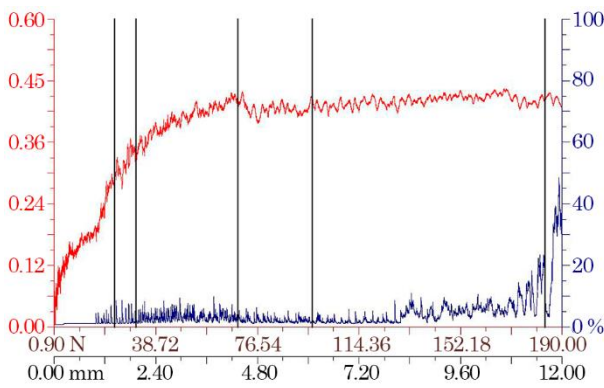
As mentioned above, the calculated  $H^3/E^2$  ratio determines the resistance of a plastic deformation material. Due to the fact that plastic deformation in materials with high hardness  $H$  and modulus  $E$  is very difficult and limited, the relatively small modulus value and, consequently, the relatively high  $H/E$  ratio is in many cases a positive factor, since in these cases the load is distributed over a larger area.

Using the relationship between  $H$ ,  $E$  and  $H^3/E^2$ , it is also possible to predict the relationship between film cracking and viscosity [19]. Generalization of the results of data analysis given in Table 2 allows to assert that the obtained coatings are characterized by amorphous crystal structure.

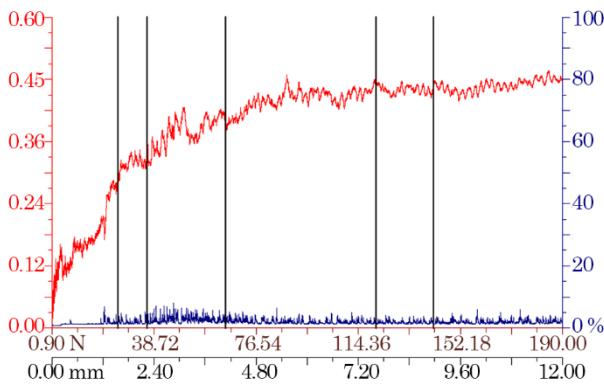
The results of sclerometric studies of adhesive and cohesive fracture of coatings on the samples of series 1 (pretreatment according to scheme 1: exposure to gas plasma without an underlaying) and series 3 (pretreatment according to scheme 3: similar exposure with the formation of an underlaying) are illustrated in Fig. 3 and Fig. 4. Minimum (critical) loads  $N$ , causing some or other changes, can be considered as quantitative indicators of adhesive interaction of the coating with the substrate:  $LC_1$  corresponds to the beginning of indenter penetration into the coating;  $LC_2$  is the mo-

ment of first crack appearance in the coating, cohesive failure;  $L_{C3}$  – delamination of some areas of the coating, adhesive failure;  $L_{C4}$  – plastic abrasion of the coating to the substrate, adhesive failure;  $L_{C5}$  – coating failure and microcracks propagation in the substrate (Table 3).

Fig. 3 shows that for both variants of the indenter immersion coatings, the general nature of the change in the coefficient of friction  $\mu$  is preserved and the differences in the intensity of AE are more significant. At first (scratch length up to 1 mm, load about 15 N), there is a relatively fast growth of  $\mu$  and practically no AE. This is the stage of establishing close contact between the indenter and the surface of the coating. Fixation of this contact is accompanied by a marked increase in  $\mu$  to a value of  $\sim 0.27$  and the appearance of AE signals (load up to 23.4 N). At further increase of load on the indenter  $\mu$  continues to increase up to values  $\sim (0.42 \div 0.45)$  with noticeable AE level (scratch length up to  $4 \div 4.5$  mm).



a



b

**Fig. 3** – Sclerometric results of the samples of series 1 (a) and series 3 (b): change in the friction coefficient (red) and acoustic emission (blue) over the indenter

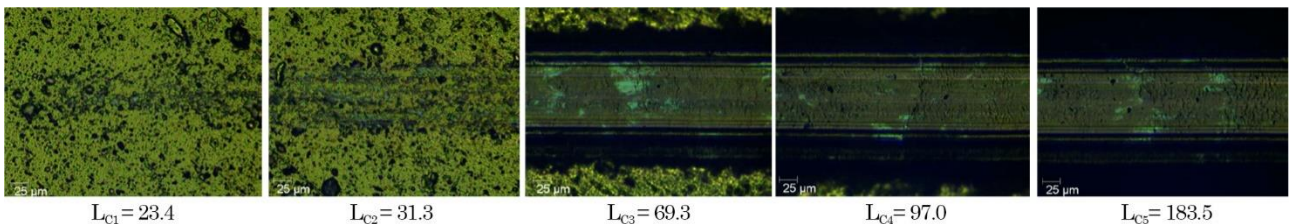


**Fig. 4** – Scratch areas on sample of series 1 at different indenter loads

After this moment and up to the end of loading  $\mu$  practically does not change for sample 1 ( $\mu_{max} = 0.46$ , Fig. 3a) and slightly grows for sample 3 ( $\mu_{max} = 0.49$ , Fig. 3b), and AE intensity in samples differs. After loads of about 75 N (scratch length 4.7 mm) in both samples, the AE signal level drops almost to the background level (2-3 % of the sensor sensitivity limit and the selected gain) with some noticeable bursts and remains that way for sample 3 until the end of the test. For sample 1, when the load reaches about 120 N, there is a noticeable increase in AE level with individual peaks 2-3 times higher than the background. After 170 N, AE level grows exponentially, and the intensity of individual peaks exceeds the background by dozens of times, which indicates the development of defects in the sample, primarily – microcracks.

The analysis of data on critical loads (Table 3) shows that  $L_{C2}$  load characterizes cohesive failure of the coating, this process continues until  $L_{C3}$  load is reached, and adhesive failure begins at high loads. Adhesion strength of the obtained coatings is very high, and, for example, several times exceeds similar characteristics of (TiHfSi)N ( $L_{C5} = 55.2$  N) [20].

The values of critical loads, as well as the nature of changes in the coefficient of friction and the level of AE signal indicate a high adhesive strength of (TiZr)N/(TiSi)N coatings, which allows recommending them to improve the performance of cutting tools. The presence of an intermediate layer does not increase the resistance of these coatings to breakage, but the process of degradation of coatings runs slower and more smoothly without sharp jump changes in properties.

**Table 3** – Hardness and modulus of elasticity of nanocomposite (Ti Zr)N/(TiSi)N coatings

Series number	Critical loads (N)				
	$L_{C1}$	$L_{C2}$	$L_{C3}$	$L_{C4}$	$L_{C5}$
1	23.4	31.3	69.3	97.0	183.5
2	22.7	28.0	43.5	99.0	184.5
3	25.3	36.0	64.1	120.8	142.1

**4. CONCLUSIONS**

The effect of surface pretreatment on the structural-phase state, mechanical properties and adhesion of vacuum-arc multilayer coatings with alternating layers (TiZr)N and (TiSi)N on 12X18H9T steel was studied experimentally. The main results can be summed up as follows:

1. The obtained (TiZr)N/(TiSi)N coatings belong to the group of materials in amorphous and amorphous-nanocrystalline states.

2. The coatings are characterized by high adhesive strength, which allows recommending them to improve the performance of cutting tools.

3. Pretreatment significantly changes the mechanical properties of coatings – hardness  $H$  and Young's modulus  $E$ : after exposure to gas plasma (series 1)  $H = 33$  GPa,  $E = 246$  GPa; after ion bombardment of cathodes with the formation of the sublayer (series 2)  $H = 25$  GPa and  $E = 19$  GPa; after exposure to gas plasma with the formation of the sublayer (series 3)  $H = 35$  GPa and  $E = 260$  GPa.

4. Adhesion strength of coatings with the sublayer does not increase, but the process of degradation of coating properties slows down. Destruction of samples

of the first series occurs at  $F = 183.5$  N; of the second – at  $F = 184.5$  N, of the third – at  $F = 142.3$  N.

5. Adhesion strength of (TiZr)N/(TiSi)N coatings is approximately 3 times higher than the adhesion strength of (TiHfSi)N coatings.

#### ACKNOWLEDGEMENTS

This work was done under the aegis of Ukrainian state budget programs «Evolution of Structure and Properties of Vacuum-Arc Multi-Component Nitride Coatings» (Registration Number 0118U002028), «Physical bases of adhesive interaction of multi-component coatings with instrumental substrate» (Registration number № 0119U002523).

#### REFERENCES

1. A.D. Pogrebnjak, O.M. Ivashishin, V.M. Beresnev, *Usp. Fiz. Met.* **17**, 1 (2016).
2. S.A. Klimenko, V.M. Beresnyev, A.S. Manokhin, M.O. Azaryenkov, S.V. Lytovchenko, P.A. Srebnyuk, A.H. Naydenko, O.S. Makovyts'kyu, Yu.Ye. Ryzhov, O.I. Kohay, Pat. 120712, Ukraina, MPK(2006): C23C 14/06, opubl. 27.01.2020, byul. № 2/2020 [In Ukrainian].
3. Yin-Yu Chang, Hung Chang, Liang-Jhan Jhao, Chih-Cheng Chuang, *Surf. Coat. Tech.* **350**, 1071 (2018).
4. Lei Wang, Liuhe Li, Guodong Li, Quansheng Ma, *Coatings*. **9**, 209 (2019).
5. O.V. Mihal, O.V. Moroz, R.I. Starovoytov, S.V. Lytovchenko, B.A. Mazilin, L.O. Pliushyn, *Probl. At. Sci. Tech.* **5** (117), 126 (2018).
6. S.V. Lytovchenko, B.A. Mazilin, V.M. Beresnev, V.A. Stolbovoy, M.G. Kovalyova, E.V. Kritsyna, I.V. Kolodiy, O.V. Glukhov, L.V. Malikov, *J. Nano-Electron. Phys.* **10**, No 5, 05041 (2018).
7. V.M. Lunev, O.V. Nemashkalo, *Phys. Surf. Eng.* **8** No 1, 64 (2010).
8. W.C. Oliver, G.M. Pharr, *J. Mat. Research.* **7**, 1564 (1992).
9. H. Ichimura, Y. Ishii, *Surf. And Coat. Techn.* **165**, 1 (2003).
10. H. Dong, *Tribological Properties of Titanium-based Alloys – Surface Engineering of Light Alloys. Aluminium, Magnesium and Titanium Alloys* (Woodhead Publishing Series in Metals and Surface Engineering: 2010).
11. E. Rabinowicz, *Friction and Wear of Materials*. (Wiley: New York: 1995).
12. A. Leyland, A. Matthews, *Wear* **246**, 1 (2000).
13. N.V. Novikov, M.A. Voronkin, S.N. Dub, I.N. Lupich, V.G. Malogolovets, B.A. Maslyuk, G.A. Podzyarey, *Diamond Related Mater.* **6**, 574 (1997).
14. S.A. Firstov, V.F. Gorban, É.P. Pechkovskii, N.A. Mameka, *Materialovedeniye* No 11, 26 (2007).
15. A.D. Pogrebnjak, A.P. Shpak, N.A. Azarenkov, V.M. Beresnev, *Phys. Usp.* **52**, 29 (2009).
16. S. Veprek, *J. Vac. Sci. Tech.* **17**, 2401 (1999).
17. J. Musil, *J. Vac. Sci. Technol. A* **28**, No 2, 244 (2010).
18. V.F. Gorban, N.A. Mameka, É.P. Pechkovskii, S.A. Firstov, *Sb. dokladov Khar'kovskoy nanotekhnologicheskoy assamblei, T. 1. Nanostrukturnyye material*, 52 (Kharkov: NSC KIPT: 2007).
19. J. Musil, M. Jirout, *Surf. Coat. Tech.* **201**, 5148 (2007).
20. A.D. Pogrebnjak, V.M. Beresnev, A.A. Demianenko, V.S. Baidak, F.F. Komarov, M.V. Kaverin, N.A. Makhmudov, D.A. Kolesnikov, *Phys. Solid State* **54**, 1882 (2012).

#### Адгезійна міцність нанокompозитних покриттів TiZrN/TiSiN на підкладці зі сталі з перехідним підшаром

В.М. Береснев<sup>1</sup>, С.В. Литовченко<sup>1</sup>, Б.О. Мазілін<sup>1</sup>, Д.В. Горох<sup>1</sup>, В.О. Столбовой<sup>1,2</sup>, Д.А. Колесніков<sup>3</sup>, І.В. Колодій<sup>2</sup>, С. Жанисов<sup>4</sup>

<sup>1</sup> Харківський національний університет імені В.Н. Каразіна, майдан Свободи, 4, 61000 Харків, Україна

<sup>2</sup> Національний науковий центр «Харківський фізико-технічний інститут» НАН України, вул. Академічна, 1, 61108 Харків, Україна

<sup>3</sup> Белгородський державний національний дослідницький університет, вул. Перемоги, 85, 308015 Белгород, Російська Федерація

<sup>4</sup> Східно-Казахстанський державний технічний університет імені Д. Серікбаєва, вул. Протозанова, 69, 070004 Усть-Каменогорськ, Республіка Казахстан

Вивчено вплив попередньої обробки поверхні на адгезійні властивості вакуумно-дугових покриттів TiZrN/TiSiN на підкладках сталі 12X18H9T. Багатошарові покриття отримували при розпилюванні двох катодів складів (мас. %) 75 Ti + 25 Zr та 94 Ti + 6 Si в одному технологічному циклі з попередньою обробкою, яка могла включати очистку зразків газовою плазмою в двоступеневому газовому розряді або іонним бомбардуванням при дуговому розпиленні катодів, осадження на підкладку підшару при дуговому розпиленні катодів, а також комбінації цих варіантів очищення з нанесенням підшару. При дослідженнях складу, структури і властивостей отриманих композитів «покриття-підкладка» використовували рентгенівський аналіз, електронну мікроскопію, склерометрію і вимірювання мікротвердості. Виявлено особливості деформації і деградації покриттів, сформованих після різних варіантів попередньої підготовки зразків. Величини критичних навантажень при

динамічному індентуванні покриттів, зміни при цьому коефіцієнта тертя і рівня сигналу акустичної емісії свідчать про високу адгезійну міцність покриттів (TiZr)N/(TiSi)N, що дозволяє рекомендувати їх для підвищення експлуатаційних характеристик різального інструменту. Наявність проміжного підшару не підвищує стійкість даних покриттів до руйнування, однак уповільнює процес деградації покриттів і згладжує різкі стрибкоподібні зміни властивостей.

**Ключові слова:** Вакуумно-дугові покриття, Адгезійна міцність, Багатошарові покриття, Попередня підготовка, Плазмовий нагрів, Проміжний підшар.